Time Domain Noise Analysis of Oversampled CMOS Image Sensors

Boyd Fowler, Andreas Suess, Mathias Wilhelmsen and Liang Zuo

OmniVision Technologies, 4275 Burton Drive, Santa Clara, CA 95054 USA

***Abstract*—In this paper we analyze the effectiveness of four oversampled techniques on the read noise performance of CMOS image sensors. We compare correlated multiple sampling (CMS), noise optimized correlated multiple sampling (NOCMS), skipper multiple sampling (SMS) and noise optimized skipper multiple sampling (NOSMS) using model parameters from two sensors. We verify the presented model against CMS measurements. We point out that floating diffusion (FD) leakage current becomes a dominant noise factor in CMS, which NOCMS can greatly reduce. Finally, we conclude that SMS and NOSMS have more potential to further reduce read noise than CMS or NOCMS.**

I. Introduction

Read noise is a fundamental limitation for image sensors under low light conditions. CMS has gained increasing popularity for read noise reduction [1]–[3]. Research for uncooled and fast noise reduction is ongoing. In this paper we will investigate noise reduction techniques based on oversampling to determine which one offers the best opportunity to achieve electron counting operation.

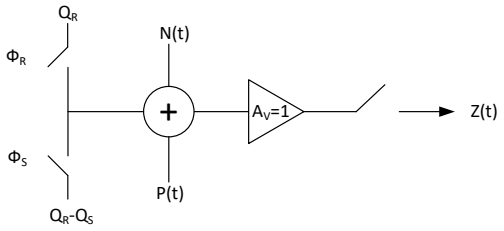

Figure 1. Model block diagram

Fig. 1 shows a simplified linearized block diagram of a CIS readout from the pixel to the column level ADC. Here, $Z(t)$ denotes the ADC sample, Q_R, Q_S are the input referred reset and signal charges, Φ_R, Φ_S are the signals determining if a reset or signal sample is measured, $N(t)$ and $P(t)$ are random processes modeling read noise and FD leakage and A_V is the conversion gain.

The first oversampling technique is CMS as described in [1]–[3]. Part a) of Fig. 2 illustrates its voltage level waveform at the input of the column level ADC. The circles represent the ADC sample points. The second technique is a variant of CMS - NOCMS, where the difference samples X_i (cf. Eq. 4) are arranged in a specific order and weighted before summation $Y = \sum_{i=1}^{N} \alpha_i \cdot X_i$ based on the noise statistics of the data [4]–[7]. This is illustrated in part b) of Fig. 2. Note that in the case where

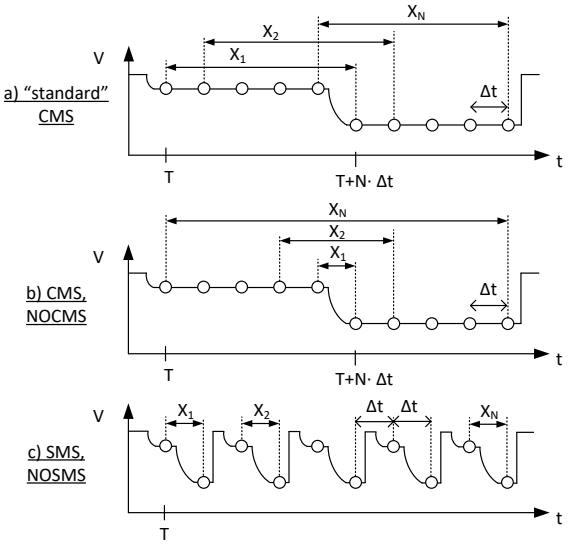

Figure 2. Oversampling waveforms - Note that X_i describes the difference of reset and signal sample. The figure illustrates the pairings of said reset and signal samples.

all weights $\alpha_i = 1/N$ both methods are equal from a stochastic point of view. For this reason we will focus on the pairing depicted in b) for the remainder of the article.

Both of these techniques assume a standard floating diffusion amplifier at the pixel. The next two techniques assume that charge can be moved at the pixel level, for example in a floating gate amplifier or skipper amplifier [8], [9], to enable a sequence of non-destructive reset and signal measurements over and over again as shown in part c) of Fig. 2. These two read out techniques are SMS [9] and NOSMS [10]. The only difference between the two techniques is that NOSMS uses a weighted sum based on the noise statistics of the data just like NOCMS.

In Section II we describe our simplified time domain readout model and derive the read noise for oversampled systems. In Section III optimal weights for NOCMS and NOSMS are derived. In Section IV we present how we derive noise models based on measurements of two sensors and in Section V we present noise power as a function of oversampling ratio for the four techniques based on white noise and the models presented in Section IV. Finally in Section VI we present summary conclusions.

II. Oversampling Theory

Earlier publications showed empirically that, e.g. X_1, X_2 should be stronger weighted than X_{N-1}, X_N due to potentially higher correlation of signal and reset sample [4], [5], [10]. Only recently [6], [7] presented mathematical attempts towards a noise optimization. However, this approach used expensive pixel-level optimization. We present a model that allows a more cost efficient implementation.

For further derivations sampling conditions are defined:

$$Z(t) = A_V \cdot \begin{cases} N(t) - P(t) + Q_R \text{ for } t \in T_R \\ N(t) - P(t) + Q_R - Q_S \text{ for } t \in T_S \end{cases} \tag{1}$$

$$T_{\mathrm{S}} = \begin{cases} \{t_{S-i} = T + (N + i - 1) \cdot \Delta t \\ \quad |i = \{1, \ldots, N\}\} \text{ for CMS, NOCMS} \\ \{t_{S-i} = T + (2i - 1) \cdot \Delta t \\ \quad |i = \{1, \ldots, N\}\} \text{ for SMS, NOSMS} \end{cases} \tag{2}$$

$$T_{\mathrm{R}} = \begin{cases} \{t_{R-i} = T + (N - i) \cdot \Delta t \\ \quad |i = \{1, \ldots, N\}\} \text{ for CMS, NOCMS} \\ \{t_{R-i} = T + (2i - 2) \cdot \Delta t \\ \quad |i = \{1, \ldots, N\}\} \text{ for SMS, NOSMS} \end{cases} \tag{3}$$

$$\begin{aligned} X_i &= A_V^{-1} \cdot [Z(t_{R-i}) - Z(t_{S-i})], t_{S-i} \in T_{\mathrm{S}}, t_{R-i} \in T_{\mathrm{R}} \\ &= Q_S + P(t_{S-i}) - P(t_{R-i}) + N(t_{R-i}) - N(t_{S-i}) \end{aligned} \tag{4}$$

where T_R and T_S are the sets of all reset and signal timepoints and X_i correspond to the difference samples. Using Eq. 2 to Eq. 4 it directly follows that

$$E[X_i|p_{m,n}] = Q_S + \frac{I_d}{q} \cdot \Delta t \cdot \begin{cases} 2i - 1 \text{ for CMS, NOCMS} \\ 1 \text{ for SMS, NOSMS} \end{cases} \tag{5}$$

where $E[\cdot|p_{m,n}]$ denotes conditional expectation of a pixel at location m, n. This results in a dark current related bias $b_{|p_{m,n}}$ in $Y = \sum_{i=1}^{N} \alpha_i \cdot X_i$ which for NOCMS also depends on the choice of weights $\boldsymbol{\alpha}$. Forcing $\sum_{i=1}^{N} \alpha_i = 1$ and subtracting the average bias $E[b]$ from Y yields a bias-free estimator $\tilde{Y}$ of Q_S:

$$\tilde{Y} = \left(\sum_{i=1}^{N} \alpha_i X_i \right) - E[b] \tag{6}$$

$$b_{|p_{m,n}} = \begin{cases} \left(\frac{I_d}{q}\right) \cdot \Delta t \cdot N \text{ for CMS} \\ \left(\frac{I_d}{q}\right) \cdot \Delta t \cdot [\sum_{i=1}^{N} \alpha_i \cdot (2i - 1)] \\ \qquad\qquad \text{for NOCMS} \\ \left(\frac{I_d}{q}\right) \cdot \Delta t \text{ for SMS, NOSMS} \end{cases} \tag{7}$$

$$E[\tilde{Y}|p_{m,n}] = Q_S + b_{|p_{m,n}} - E[b] \tag{8}$$

$$\begin{aligned} E[\tilde{Y}] &= E[E(\tilde{Y}|p_{m,n})] \\ &= Q_S - E[b] + \underbrace{E[b_{|p_{m,n}}]}_{=E[b]} = Q_S \end{aligned} \tag{9}$$

with $E[\cdot]$ as the total expectation.

The error between $\tilde{Y}$ and the true value Q_S can be measured quadratically:

$$\begin{aligned} &E[(\tilde{Y} - Q_S)^2] = \sigma_{\tilde{Y}}^2 = \sigma_Y^2 \\ &= \left(\sum_{i=1}^{N} \sum_{j=1}^{N} \alpha_i \cdot \alpha_j \cdot R_{X-Q}(i,j) \right) - \left(\sum_{i=1}^{N} \alpha_i \cdot E[X_i] \right)^2 \end{aligned} \tag{10}$$

where σ_Y^2 and $\sigma_{\tilde{Y}}^2$ are the total variances of Y and $\tilde{Y}$, and $R_{X-Q}(i,j) = E[E[X_i \cdot X_j|p_{m,n}]]$ is the expected autocorrelation function across all pixels. Section IV addresses how we model and estimate R_{X-Q} and $E[I_d]$ which explains $E[X_i] = E[E[X_i|p_{m,n}]]$ through Eq. 5.

III. Noise optimization of CMS and SMS

Using Eq. 4 one can derive the relation between the Q_S-dependent R_{X-Q} and a signal-free R_X:

$$\begin{aligned} R_{X-Q}(i,j) &= E[X(i) \cdot X(j)] \\ &= 2 \cdot Q_S \cdot (Q_S + E[b]) + R_X(i,j). \end{aligned} \tag{11}$$

With that follows that the goal function Eq. 10 yields optimal weights $\boldsymbol{\alpha}^*$ that are not dependent on Q_S:

$$\begin{aligned} \sigma_{\tilde{Y}}^2 &= E[Y^2] - (E[b] + Q_S)^2 \\ &= \sum_{i=1}^{N} \sum_{j=1}^{N} \alpha_i \cdot \alpha_j \cdot R_{X-Q}(i,j) - (E[b] + Q_S)^2 \\ &= E[Y_{|Q_S=0}^2] - (E[b])^2 + Q_S^2. \end{aligned} \tag{12}$$

The resulting optimization problem Eq. 13 with $E[\tilde{Y}^2]$ being convex[1] and the affine equality constraint $\mathbf{1}^T\boldsymbol{\alpha} = 1$ results in $\boldsymbol{\alpha}^*$ describing a minimum which we compute using the Lagrange function $L(\boldsymbol{\alpha}, \lambda)$ with the Lagrange multiplier λ:

$$\boldsymbol{\alpha}^* = \arg\min_{\boldsymbol{\alpha} \in \chi} E[\tilde{Y}^2], \chi = \left\{ \boldsymbol{\alpha} \in \mathbb{R}^N \,\middle|\, \sum_{i=1}^{N} \alpha_i = 1 \right\} \tag{13}$$

$$L(\boldsymbol{\alpha}, \lambda) = E[\tilde{Y}^2] + \lambda \cdot \left(\sum_{i=1}^{N} \alpha_i - 1 \right) \tag{14}$$

$$\begin{aligned} \frac{\partial L}{\partial \alpha_i} &= E\left[2 \cdot (Y - E[b]) \cdot \frac{\partial}{\partial \alpha_i} (Y - E[b]) \right] + \lambda \\ &= 2 \cdot E[Y \cdot X_i] - 2 \cdot E[b] \cdot E[X_i] + \lambda \end{aligned} \tag{15}$$

Now writing out $Y = \sum_{i=1}^{N} \alpha_i \cdot X_i$ and rearranging the set of equations while using $\mathrm{cov}_{\mathrm{X}}(i,j) = R_X(i,j) - E[X(i)] \cdot E[X(j)]$ yields Eq. 16. If $\mathbf{H}_L$ is invertible (non-singular), then $\boldsymbol{\alpha}^*$ is a unique global minimum:

[1] With $\boldsymbol{\alpha}[\xi] = \xi \cdot \boldsymbol{\alpha}_1 + [1 - \xi] \cdot \boldsymbol{\alpha}_2 \; \forall \boldsymbol{\alpha}_1, \boldsymbol{\alpha}_2 \in \mathbb{R}^N, \boldsymbol{\alpha}_1 \neq \boldsymbol{\alpha}_2$ $\xi \in (0,1)$ one can show that $E[\tilde{Y}^2]$ is convex as $0 \geq E[\tilde{Y}^2(\boldsymbol{\alpha}[\xi])] - \xi \cdot E[\tilde{Y}^2(\boldsymbol{\alpha}_1)] - [1 - \xi] \cdot E[\tilde{Y}^2(\boldsymbol{\alpha}_2)]$ $= \underbrace{[\xi^2 - \xi]}_{<0 \; \forall \xi \in (0,1)} \cdot \underbrace{(\boldsymbol{\alpha}_1 - \boldsymbol{\alpha}_2)^T \mathbf{cov}_X (\boldsymbol{\alpha}_1 - \boldsymbol{\alpha}_2)}_{=E\left[([\boldsymbol{\alpha}_1 - \boldsymbol{\alpha}_2]^T \mathbf{X})^2\right] \geq 0}$ holds.

$$\begin{bmatrix}0\\ \vdots\\ 0\\ 1\end{bmatrix} = \underbrace{\begin{bmatrix}\mathrm{cov_X}(1,1) & \dots & \mathrm{cov_X}(1,N) & 1\\ \vdots & \ddots & \vdots & \vdots\\ \mathrm{cov_X}(N,1) & \dots & \mathrm{cov_X}(N,N) & 1\\ 1 & \dots & 1 & 0\end{bmatrix}}_{=\mathbf{H}_L} \cdot \begin{bmatrix}\alpha_1^*\\ \vdots\\ \alpha_N^*\\ \lambda/2\end{bmatrix}, \tag{16}$$

IV. Underlying Noise Models

Note that from Eq. 2 and Eq. 3 it follows that:

$$\begin{aligned}
|t_{S-i} - t_{S-j}| &= \begin{cases}\Delta t \cdot |j-i| \text{ for CMS, NOCMS}\\ 2\cdot\Delta t\cdot|j-i| \text{ for SMS, NOSMS}\end{cases}\\
|t_{S-i} - t_{R-j}| &= \begin{cases}\Delta t \cdot |j+i-1| \text{ for CMS, NOCMS}\\ \Delta t\cdot|2(j-i)+1| \text{ for SMS, NOSMS}\end{cases}\\
|t_{S-i} - t_{S-j}| &= |t_{R-i} - t_{R-j}|\\
|t_{S-i} - t_{R-j}| &= |t_{S-j} - t_{R-i}| \text{ for CMS, NOCMS}\\
|t_{S-i} - t_{R-j}| &\neq |t_{S-j} - t_{R-i}| \text{ for SMS, NOSMS}
\end{aligned} \tag{17}$$

We assume that the read noise can be modeled as a superposition of Lorentzian Random Telegraph Signal (RTS) noise sources with time-constants τ_k [11], [12]

$$R_N(t_1,t_2) = \sum_{k=1}^{K} c_k \cdot \exp\left(-|t_1-t_2|/\tau_k\right). \tag{18}$$

This inherently assumes that the low-pass-filtering characteristic of the readout circuit has a much smaller time-constant than the Lorentzians. Note, it can be shown that for a first order filter white noise - e.g. thermal noise - also takes the shape of a Lorentzian which in this case determines the smallest time-constant.

$$\begin{aligned}
R_X(i,j) &= \left(\frac{I_d}{q}\right)^2 \cdot [2i-1][2j-1]\cdot(\Delta t)^2\\
&+ \left(\frac{I_d}{q}\right)\cdot\Delta t\cdot(2\cdot\min[i,j]-1)\\
&+ \sum_{k=1}^{K} c_k \cdot \left[2\cdot e^{-\frac{\Delta t\cdot|j-i|}{\tau_k}} - 2\cdot e^{-\frac{\Delta t\cdot|j+i-1|}{\tau_k}}\right]\\
&\qquad\qquad \text{for CMS, NOCMS}\\
&= \left(\frac{I_d}{q}\right)^2 (\Delta t)^2 + \delta(i,j)\cdot\left(\frac{I_d}{q}\right)\cdot\Delta t\\
&+ \sum_{k=1}^{K} c_k \cdot \left[2\cdot e^{-\frac{2\Delta t\cdot|j-i|}{\tau_k}} - e^{-\frac{\Delta t\cdot|2(i-j)+1|}{\tau_k}}\right.\\
&\qquad \left. - e^{-\frac{\Delta t\cdot|2(j-i)+1|}{\tau_k}}\right]\\
&\qquad\qquad \text{for SMS, NOSMS}
\end{aligned} \tag{19}$$

Eq. 19 results from the autocorrelation function of a shot noise process $R_P(t_1,t_2) = \lambda^2(t_1-t_0)(t_2-t_0) + \lambda\cdot\min[t_1-t_0, t_2-t_0]$ with $t_0 = T$ (cf. Fig. 2) and $\lambda = I_d/q$ and using $E[N(t_i)\cdot P(t_j)] = 0$ together with Eq. 4 and Eq. 17.

We estimate the model parameters I_d and $\mathbf{c}$ from CDS samples [13] of two image sensors *A* and *B* using

$$\begin{aligned}
X &= A_V^{-1}\cdot[Z(t_0) - Z(t_0+t)]\\
&= Q_S + P(t_0,t_0+t) + N(t_0) - N(t_0+t)\\
\sigma^2_{X|p_{m,n}}(t) &= 2\cdot R_{N|p_{m,n}}(0) - 2\cdot R_{N|p_{m,n}}(t) + \frac{I_d}{q}\cdot t\\
&= 2\cdot\sum_{k=1}^{K} c_k\cdot[1-\exp(-t/\tau_k)] + I_d\cdot t/q\\
[\mathbf{c},\boldsymbol{\tau},I_d] &= \arg\min_{\tilde{\mathbf{c}},\tilde{\boldsymbol{\tau}},\tilde{I}_d}\sum_{l=1}^{L}\left|S_X^2(t_l) - \sigma^2_{X|p_{m,n}}(t_l)\right|^2
\end{aligned} \tag{20}$$

with the sample variance $S_X^2(t_l)$. For Sensor *A* we used t_l from 10 µs to 140 µs and for Sensor *B* 3 µs to 120 µs. We assume that the Lorentzian time-constants can only exhibit a predefined set of values, e.g. $\boldsymbol{\tau} = [1\,\text{ms}, 310\,\mu\text{s}, 100\,\mu\text{s}, 31\,\mu\text{s}, 10\,\mu\text{s}, 3.1\,\mu\text{s}, 1\,\mu\text{s}]$. Individual pixels may not exhibit all RTS time-constants. Hence, for a predefined maximum amount of Lorentzians per pixel (here 7) we permutate through all combinations ($2^7 - 1 = 127$) starting from the smallest time-constant and compute the least-squares fit of $\mathbf{c}, I_d$. We then force positive weights by $\mathbf{c} = \max(\mathbf{c}, 0)$. If new parameters reduce the average absolute fitting error and increase $\sum_k c_k$ the optimum parameters are updated. The last condition avoids overfitting. This procedure is executed until all permutations have been compared. Fig. 3 and Fig. 4 show example distributions of $\mathbf{c}$ and I_d after pixel level regression. The reason that the $1-\text{CDF}$ curves do not reach 1 in logscale is that some pixels do not exhibit these time-constants. Hence, the difference to 1 gives rise to the significance of τ_k, c_k.

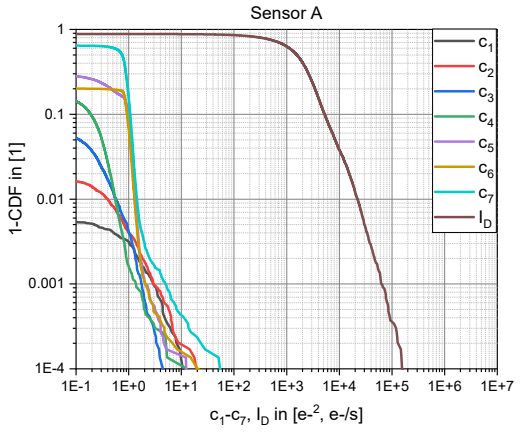

Figure 3. Fitting parameters of sensor *A*.

V. Results

Sensor *A* implements CMS and hence, is used to verify the model presented in this paper. Here, we varied Δt of 10 µs, 20 µs, 40 µs and 80 µs. For each Δt setting we

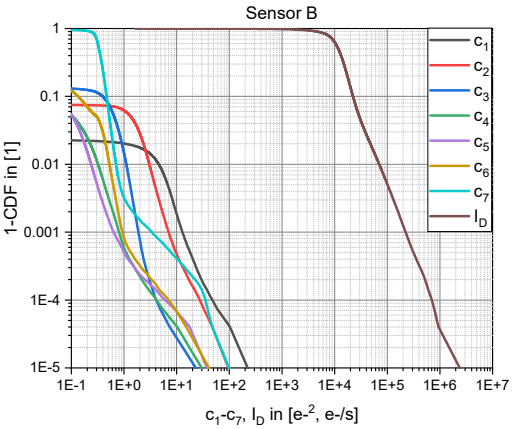

Figure 4. Fitting parameters of sensor *B*.

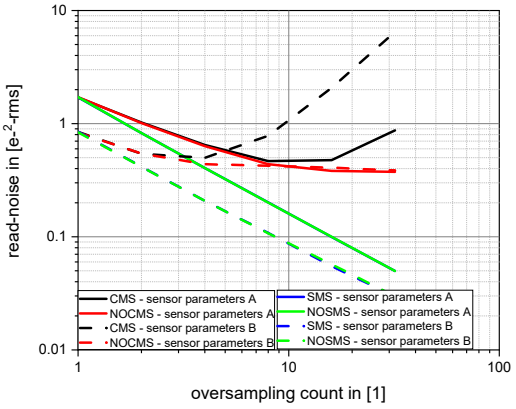

Figure 6. Oversampling results based on model from sensor *A* and *B*.

acquiring read noise data for x1, x2 and x4 oversampling. Fig. 5 demonstrates a reasonable resemblance of model and measurements as long as the total read-time $N \cdot \Delta t$ does not exceed the range of t_l used to fit the model as described in Sec. IV. We determined $\sigma^2_{\tilde{Y}}$ using the law of total variance of Monte-Carlo trials of $\mathbf{c}, I_d | p_{m,n}$:

$$\sigma^2_{\tilde{Y}} = \boldsymbol{\alpha}^T \cdot E[\mathbf{cov}_{X|p_{m,n}}] \cdot \boldsymbol{\alpha} + \mathrm{var}(E[\tilde{Y}|p_{m,n}]) \quad (21)$$

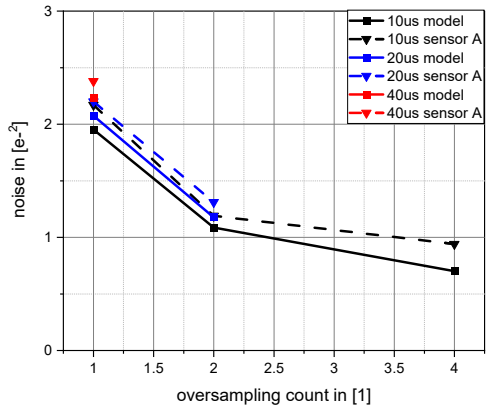

Figure 5. CMS model based on CDS samples of sensor *A* vs. CMS measurements of sensor *A*.

Having verified the validity of the presented model we now compare CMS, NOCMS, SMS and NOSMS in Fig. 6. We calculate $\boldsymbol{\alpha}^*$ based on the expected covariance (cf. Eq. 16). Again we use Monte-Carlo trials and law of total variance to determine $\sigma^2_{\tilde{Y}}$.

Here, we selected a Δt of $4\,\mu\mathrm{s}$ and assumed that the conversion gain of CMS and SMS can be matched. Depending on the sensor specifics, FD leakage can become the dominant noise source in CMS leading to a significant increase in read noise for, e.g. sensor *B*. It can be seen that NOCMS is greatly helpful in reducing the impact of FD dark current or flicker noise such that instead of yielding a potentially narrow localized noise minimum, read noise can be further reduced until eventually a plateau is reached. The actual read noise minimum was reduced by $20\,\%$ for sensor *A* and $23\,\%$ for sensor *B* by using noise optimization. It can be seen that due to the high correlation of the signal and read samples noise-optimization is less helpful for skipper mode-readout. Note that if one could design a skipper mode readout structure with sufficiently high conversion gain while keeping the buried memory storage and sense node leakage currents sufficiently small, SMS may have a competitive advantage in reaching ultra-low read noise over CMS or NOCMS. Note for comparison that [14] reported a PPD with floating gate-readout structure in a $0.18\,\mu\mathrm{m}$ technology reaching a conversion gain of $38\,\mu\mathrm{V}/\,\mathrm{e}^-$. [15] presented TCAD simulations of a similar PPD device with Skipper readout achieving possibly $85\,\mu\mathrm{V}/\,\mathrm{e}^-$.

VI. Conclusion

We presented a thorough stochastic signal analysis of oversampling noise in CMS, NOCMS, SMS and NOSMS systems. We emphasized the importance of floating diffusion dark current in sub-electron sensing devices and bring attention to the floating gate amplifier as a potential alternative for achieving ultra-low read noise.

References

[1] A.M. Fowler et al., ApJ, 353, pp. L33-L34, Apr. 1990.
[2] A.M. Fowler et al., Proc. SPIE 1991, 1541, 127-133, Nov. 1991.
[3] N. Kawai et al., IEICE Electronics Express, Vol. 2, No.13 July 2005.
[4] J.-L. Gach et al., PASP 115 1068, Sep. 2003.
[5] M. Clapp et al., Proc. SPIE 99151S, July 2016.
[6] C. Alessandri et al., MNRAS, 2016. arXiv:1511.05649.
[7] P.Q. Simbeni et al., CAE, 2019. doi: 10.1109/CAE.2019.8709288.
[8] D. Wen, IEEE JSSC, Vol. 9, No. 6 Dec. 1974.
[9] J. Janesick et al., Proc. SPIE Vol 1242, July 1990.
[10] G. F. Moroni et al., arXiv:1106.1839, June 2011.
[11] A. van der Ziel, Wiley, NY 1986.
[12] A.L. McWhorther, PhD thesis, MIT, 1955.
[13] R. Ispasoiu et al., IISW June 2009
[14] A. Krymski et al., IISW June 2015
[15] K. Stefanov et al., Sensors Vol. 20, 2020